Journal of Intelligent Systems and Internet of Things
Vol. 18, No. 02, PP. 290-303, 2026
DOI: https://doi.org/10.54216/JISIoT.180220

Improving Pedestrian Walkways for Individuals with Disabilities Using Heuristic Search Based Parameter Tuning with Deep Transfer Learning Models

Reem Alshenaifi[1,*]

[1]Department of Information Technology, College of Computer and Information Sciences, Majmaah University, Majmaah, 11952, Saudi Arabia

Email: r.alshnaifi@mu.edu.sa

Abstract

Blind and visually challenged people face the range of practical issues by undertaking outside travels as pedestrians. In the last decade, various beneficial devices is investigated and established to assist people with disabilities move independently and safely. Anomaly detection in pedestrian paths for visually impaired individuals, using remote sensing (RS), is crucial for improving pedestrian traffic flow and safety. Engineers and investigators can create efficient methods and tools with the effect of computer vision (CV) and machine learning (ML) to recognize anomalies and alleviate possible security hazards in pedestrian walkways. With recent progress in deep learning (DL) and ML fields, researchers have realised that the image recognition problem is supposed to be developed as classification problems. This paper proposes a Coati Optimization Algorithm-Based Parameter Tuning for Pedestrian Walkways with Transfer Learning Model (COAPT-PWTLM) technique. The main goal of COAPT-PWTLM technique is to provide automatic detection of pedestrian walkways for disability using advanced models. Initially, the median filtering (MF) is employed in the image pre-processing stage to eliminate the noise from an input image data. Furthermore, the SquezeNet1.1 model is utilized for feature extraction. For the classification process, the multi-layer autoencoder (MLAE) model is implemented. Finally, the modified update coati optimization algorithm (MUCOA) model adjusts the hyperparameter range of MLAE method optimally and results in improved classification performance. The experimental validation of the COAPT-PWTLM is verified on a benchmark image dataset and the outcomes are evaluated under dissimilar measures. The experimental outcome underlined the progress of the COAPT-PWTLM model over the existing models.

Received: February 22, 2025 Revised: June 01, 2025 Accepted: July 20, 2025

Keywords: Coati Optimization Algorithm; Pedestrian Walkways; Transfer Learning; Disability Individuals; Image Pre-processing

1. Introduction

In 2020, as per the world health organization (WHO), billions of people are impaired visually. For the loss of sight and vision impairment, there are several reasons, which include neurological faults from birth, age-related cataracts and uncorrected refractive mistakes [1]. For those who are suffering from vision impairment, both freedom, and self-confidence in taking day-to-day actions for existence are impacted [2]. To help visionless and visually disabled people, the assistive methods help with several activities namely identifying people, selecting dresses, differentiating banknotes and supports to navigate both outdoors and indoors [3]. However, it is much difficult for visually impaired people (VIP) to explore and visit places that is new and uncommon. Normal people may rely on their vision in finding locations; they have to depend on further senses to find places properly [4]. People with disability face difficult issues when they navigate public outdoor zones on their foots, where easy tasks like road crossing, avoiding obstacles and utilizing public transport have severe threats and troubles which

in turn threaten their security, confidence and freedom of VIP which limits their capability to engage in society [5].

Now, the development of technology permits the methods of navigating with vision disability people. Global positioning system (GPS) technology is developed to navigate outdoors and incorporated together with geographic information systems (GIS) for the pedestrian walkways. Presently, the availability of low-cost image acquisition methods and the convenient unmanned RS vehicles (UAVs) has made RS imaging (RSI) more appropriate and common [6]. It has possibility of obtaining extended variety of great-quality RSI without detailed plan and significant volume of time [7]. Various tasks adopted RSI such as urban studies, cartography, landscape archaeology and precise agriculture over a while. In RSI, for the classification and detection of vehicles, one efficient implementation is needed. It is adopting gradually for smarter transport for parking space allocation, traffic flow estimation, pedestrian walkways, vehicle identification, etc [8]. For transportation and vehicle-related applications, RSI has become the upcoming trend. In recent times, vehicle identification in RSI had been employed widely in various areas and it attracts significant attention [9]. With the recent developments in DL and ML strategies, it is now able to achieve greater object-detecting rates in cluttered acts. DL and ML are the sub-fields of artificial intelligence (AI) that focus on the statistical methods and algorithm designs, that lets computers study and generate predictions without programming explicitly [10].

This paper proposes a Coati Optimization Algorithm-Based Parameter Tuning for Pedestrian Walkways with Transfer Learning Model (COAPT-PWTLM) technique. The main goal of COAPT-PWTLM technique is to provide automatic detection of pedestrian walkways for disability using advanced models. Initially, the median filtering (MF) is employed in the image pre-processing stage to eliminate the noise from an input image data. Furthermore, the SquezeNet1.1 model is utilized for feature extraction. For the classification process, the multi-layer autoencoder (MLAE) model is implemented. Finally, the modified update coati optimization algorithm (MUCOA) model adjusts the hyperparameter range of MLAE method optimally and results in improved classification performance. The experimental validation of the COAPT-PWTLM is verified on a benchmark image dataset and the outcomes are evaluated under dissimilar measures.

2. Literature Survey

Talaat et al. [11] presented SafeStride, an innovative model intended to permit VIPs over real-world navigation assistance and obstacle detection. SafeStride functions around 5 interconnected stages: path planning, sensor data acquisition, obstacle detection, data pre-processing, guidance and feedback. An integration of cameras, ultrasonic sensors and inertial measurement units (IMUs) feed complete ecological data into the method, allowing precise safe path planning and obstacle detection. Nasabeh et al. [12] projected an extension of the MoSIoT structure, combining the YOLO-v8 CNN for accurate OD and specialized decision layer to enhance ecological awareness. Furthermore, sophisticated distance measurement models are integrated to offer vital data on object proximity. This technique determines improved adaptability and efficacy through different settings employing robust regularization and TL methodologies. Jeong et al. [13] advanced an eXtended Reality (XR) glasses-based walking assistance method. This method employs the YOLOv8n DL technique to identify walkable regions, public transport resources, and obstacles in real world and offer relevant guidance to the user. The key elements of these methods are Android-based smartphones and Xreal light smart glasses, which are performed over a mobile application advanced by employing the Unity game engine.

Chowdhury et al. [14] develop an innovative deep-edge solution employing CV. This novel presents a different innovative tactile footpath dataset of Dhaka encompassing diverse regions of cities. In addition, current sophisticated DNN for OD is adjusted and examined utilizing this dataset. HBFN methodology is advanced to offer navigation direction, which is obstacle-free, and safe, which is then employed in a smartphone application. Choi et al. [15] evolve a driving support method to prevent accidents and improve user security. This method combines front-facing camera and ultrasonic sensors to identify difficulties and deliver real-world warnings. The presented model functions individually for stable server communication and utilizes embedded hardware for environmental recognition and rapid object detection, guaranteeing instant guidelines in multiple set-ups. This technique also employs yolo-v8 approach. So, the YOLO technique was sped up through inference on the specialized hardware in the experimentation. Lee et al. [16] projected a method for VIP in walking surroundings. It integrates OD employing YOLO-v5 and cautionary sentence generation with KoAlpaca. A pilot test including healthy and visually impaired individuals is performed. Ikram et al. [17] introduce FusionSight, a novel multi-modal fusion technique, which combines image and radar data. This method employs an Arduino Uni micro-controller for transmission and data acquisition. For imaging data, the ViT was utilized to eliminate higher-level features. Simultaneously. Radar data is processed employing a CNN to remove temporal and spatial aspects. For integrating these multiple modalities, a feature fusion multi-modal transformer (FFMA) was employed. The unified aspects were categorized into 4 classes “close, far, moving and fast-moving” utilizing a FFNN.

3. Methodology

In this paper, the COAPT-PWTLM technique is proposed. The main goal of COAPT-PWTLM technique is to provide automatic detection of pedestrian walkways for disability using advanced models. Fig. 1 illustrates the entire flow of COAPT-PWTLM method.

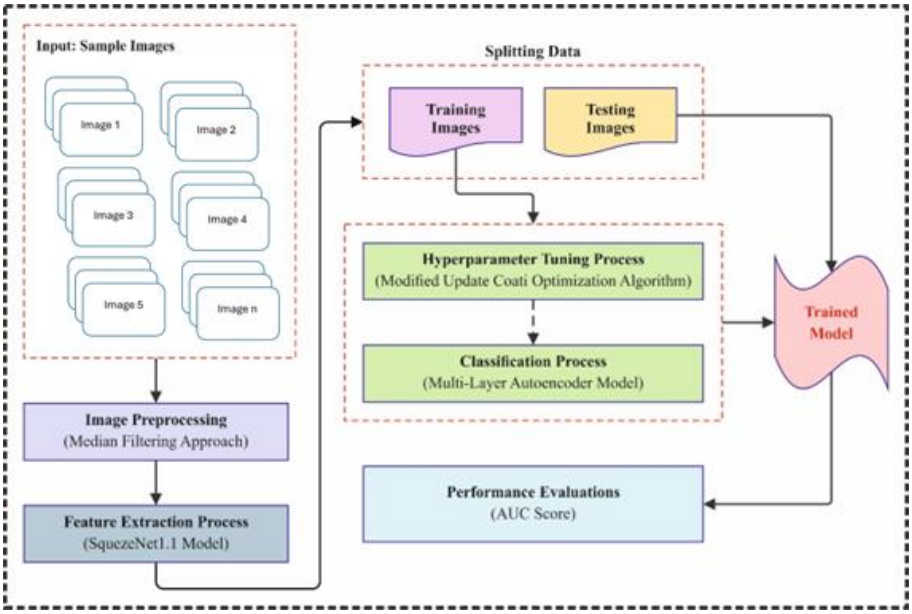

Figure 1. Overall flow of COAPT-PWTLM model

A. Image Preprocessing

Initially, the MF is used in the image pre-processing stage to eliminate the noise from an input image data. MF is an extensively applied noise reduction method in image processing, mainly for improving pedestrian walkway images [18]. It operates by substituting every value of the pixel with the median values of neighbouring pixels, successfully removing noise whereas maintaining edges. This is important to detect walkway obstacles, patterns, and cracks, enhancing availability study for people with disabilities. Once used for walkway mapping, MF aids improve visual clarity; make features such as lane markings and surface anomalies more different. Its efficiency in processing impulse noise making it a major pre-processing stage in CV methods for smart pedestrian infrastructure planning.

B. Feature Extractor using SquezeNet1.1

Besides, the SquezeNet1.1 model does the extraction of feature process. Small CNN methods, such as SqueezeNet, provide important benefits, like lowered computational demand and rapid training, making them suitable for development on resource-restricted devices [19]. Their scalability through different hardware atmospheres and capability for simplifying cloud-to-device deployment allow effective methods obtain for independent systems. In addition, they are best for memory-limited hardware such as field-programmable gate arrays (FPGAs) that acquire parallel processes inside resource-limited context. The structure presents an individual elementary unit named the fire module (FM) that acts as the basis for making effective and lightweight CNNs. The FM includes expand and a squeeze layer, all tailored for optimizing feature representation and parameter efficacy. Every module contains the activation function of rectified linear unit (ReLU) to improve nonlinearity and enable deep-network structures. The squeeze layer uses 1x1 convolutions to decrease the input channel counts, whereas the expanding layer utilizes mixture of 1x1 and 3x3 convolutions to improve the representation capability of the network. The usage of 1x1 filters in the expanding layer is important to reduce computing cost, while the addition of 3x3 filters allows the system to capture spatial local features successfully. This structure is constructed on 3 important design tactics, targeted at minimizing parameter count while preserving competitive precision.

1. SqueezeNet 1.0 and SquezeNet1.1

SqueezeNet l. 0 presented a compact structure. It encompasses a first convolutional layer (convl), 8 FMs (fire 2 to fire 9), and the last convolutional layer (conv 10). The framework combines maxpooling afterward the first convolutional layer (CL), FMs 4 and 8. To enhance efficacy, SqueezeNet l. 0 uses tactics like substituting 3x3

filters with lxl filters, utilizing lxl filters with previously 3x3 filters, and delay downsampling to recollect large activation mapping in previous layers. Based on that, SqueezeNet1.1 attains 2.4 x lower calculation and somewhat smaller parameters than SqueezeNetl.0 without disrupting precision. It decreases the filter amount in squeeze and convl layers while preserving the similar order of 8 FMs. Maxpooling is achieved afterward the first CL, FMs 3 and 5. Both structures establish the efficacy of parameter-effective model and are suitable for use on resource-limited devices.

To additionally explore the efficacy of CNN structures with even smaller parameters, presented a new variant of SqueezeNet by decreasing the FM counts:

2. SqueezeNet1.1 Variant 1 (1 FM)

This ultra-lightweight variant contains 3x3 CLs (smde 2, 64 filters) succeeded by 3x3 maxpooling layers (smde 2). The particular FM was involved that comprises an Expanding Layer and Squeeze Layer (1x1 convolution) dividing into 1xl and 3x3 CL (either with 64 filters). Afterward, the FM, 3x3 maxpooling layers (stride 2) is used. The classification layers consist of the 1x1 CL, softmax output, and a global average pooling.

3. SqueezeNet1.1 Variant 2 (2 FMs)

This variant offers a balance between representational power and efficiency. It starts with 3x3 CLs (smde 2, 64 filters) accompanied by the 3x3 maxpooling layer (smde 2). Dual FMs are incorporated, all containing Squeeze Layers (1x1 convolution) and an Expanding layer using 1x1 and 3x3 subdivisions (either with 64 filters). Afterward the FMs, a 3x3 maxpooling layer (smde 2) is utilized. The method determines softmax activations, a 1x1 CL, and global average pooling. This configuration provides enhanced feature extraction in comparison with version 1 whereas residual is computationally effective.

4. SqueezeNet1.1 Variant 3 (4 FMs)

This variant improves feature representation while preserving the structure lightweight. It starts with 3x3 CLs (64 filters, stride 2) accompanied by the 3x3 maxpooling layer (stride 2). Four FMs are involved. Every FM contains an expanding layer and a squeeze layer (1x1 convolution) by dual divisions: 1x1 and 3x3 convolutions. The initial dual FMs take 64 filters in the sections; however, the following dual FMs have 128 filters. The 3x3 maxpooling layer (stride 2) is used afterward the FMs, accompanied by the softmax activation, a 1x1 CL, and global average pooling, This version is best for applications needing high precision without an important rise in computational complexity.

C. Classification using MLAE Model

For the classification process, the COAPT-PWTLM technique deploys MLAE model. Unlike conventional methods that relies on handmade features, the ML-AE learns abstract, hierarchic representations of the input data, taking refined designs and abnormalities that are important for accurate detection of disease [20]. Its deeper structure permits it to model composite relationships inside the data. The multi-layer model enhances its capability for learning progressively composite features, making it suitable for the tasks of multi-disease classification. Generally, the ML-AE provides higher scalability, flexibility, and better performance associated with simple, single-layer AEs or conventional image classification methods.

An AE is the NN designed for compressing massive datasets by reducing the data dimensions above non-linear transformation. It comprises two stacked NN like the encoder indicated as (β_e and parameterized by (β_e and the decoder by (β_d, parameterized by θ_{enc}. The encoding endures with the input data image $u_n^{(i)} \in \mathbb{R}^{N_u}$ and delivering condensed representations $z_n^{(i)} \in \mathbb{R}^{Nz}$ in a hidden area. Nowadays, N_Z indicates the amount of hidden area variable however generally chosen $N_Z'' N_u$. As the matrix $U^{(i)}$, the hidden signs are connected at all moments in the matrix $Z^{(i)} = [z_0^{(i)}, \dots, z_{N_t}^{(i)}]^T \in \mathbb{R}^{(N_t+1)\times N_Z}$. The variable of hidden for all moments and $\mu^{(i)}$ parameter are preserved in the 3^{rd}-order tensor $Z \in \mathbb{R}^{N_\mu \times (N_t+1)\times N_Z}$, such as tensor U:

$$Z = [Z^{(1)}, \dots, Z^{(N_\mu)}]_{N_\mu \times (N_t+1)\times N_Z} \tag{1}$$

The decoder captures all $z_n^{(i)}$ as input and generates a reconstructed category of $u_n^{(i)}$ that is shown as $\hat{u}_n^{(i)}$.

$$z_n^{(i)=} \varphi_e\left(u_n^{(i)} \middle| \theta_{enc}\right)$$

$$\hat{u}_n^{(i)} = \varphi_d\left(z_n^{(i)} \middle| \theta_{dec}\right) \tag{2}$$

The AE parameters, denoted as θ_{enc} and θ_{dec}, are learned using a numeric optimization approach which decreases the L_2 dissimilarity model between the collection of reconstructed solutions $\widehat{U}$ in addition to the collection of input solution U. It is achieved by labelling the reconstruction loss as below:

$$L_{AE}(\theta_{enc}, \theta_{dec}) = \|U - \widehat{U}\|_2^2$$
$$= \frac{1}{N_\mu}\sum_{i=1}^{N_\mu}\left(\frac{1}{N_t+1}\sum_{n=0}^{N_t}\left\|u_n^{(i)} - \varphi_d(\varphi_e\left(\left(u_n^{(i)}\middle|\theta_{enc}\right)\middle|\theta_{dnc}\right)\right\|_2^2\right) \quad (3)$$

The ML-AE is the type of NN approach, which removes the latent features of the input dataset. The framework includes decoding and encoding portions. The encoding includes input and FC layers. The decoding has FC layers and output. The layer of FC processing from $x \in \mathbb{R}^{\Omega}$ to $y \in \mathbb{R}^{\Psi}$ is measured by Eq. (4):

$$y = \delta(Wx + b), \quad (4)$$

Now, $W \in \mathbb{R}^{\Psi \times \Omega}$ specifies the weighted matrix of coefficient, $\delta(\cdot)$ signifies the function of the activation, and $b \in \mathbb{R}^{\Psi}$ displays the biased term.

The AE decrease the function of loss in reducing the optimal weighted bias and coefficient in the training procedure:

$$Loss = \frac{1}{H}\sum_{i=0}^{H-1}(x_i - z_i)^2 \quad (5)$$

Here, x_i and z_i represents i^{th} output and input AE neurons; consistently, H specifies the neuron amount within the input layer. Fig. 2 illustrates the structure of MLAE.

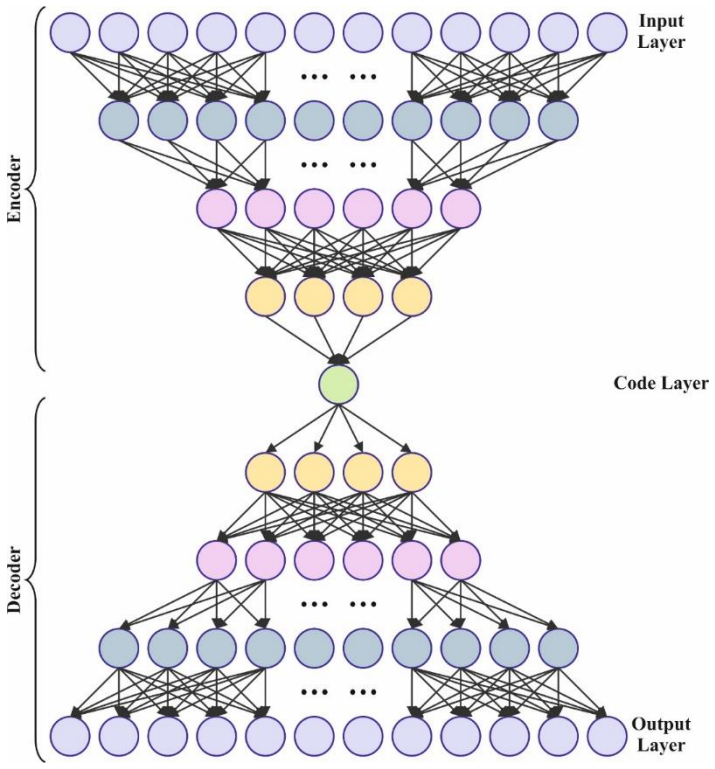

Figure 2. MLAE structure

D. Parameter Selection using MUCOA

At last, the MUCOA adjusts the hyperparameter selection of MLAE model optimally and results in improved performance. To design the previous onset plant disease prediction structure, the changed MUCOA model is designed [21]. The main goal of designing the process model is for tuning the parameters, which aid in improving the performance. Now, the novel expression is obtained to perform the process by addressing the limits in the conventional COA method. The MUCOA is mostly utilized to tune the epochs and hidden neurons of the feature extraction methods to increase the accuracy and precision values. The MUCOA is proposed by enhancing the arbitrary number in the traditional COA to acquire the best and most efficient solution. The novel random number

was computed according to the poor and the best fitness values and it is mathematically resulting in Eq. (6). The updated random number in the MUCOA aids in detecting the solution in the novel searching region. The searching ability of the MUCOA aids in avoiding the local best state. The multi-objective difficulties in the searching region are processed by the MUCOA and it contains faster convergence ability instead of the traditional methods. In detail, the parameter tuning in the MUCOA is applied to improve the feature extraction process. Also, the understand ability of the DL method used for the feature extraction is improved due to the parameter optimizer utilizing the MUCOA. In addition to its usages, this method decreases the training time that assistances in acquiring precise outcomes. The classic COA method has reached the best values in an improved way. It can provide the most suitable solutions for optimizer problems by strike the related balance between exploitation and exploration in the local search and global search. However, there is a need for multi-modal and binary types of COA.

Therefore, the novel derivative for randomly generated numbers is developed in this method. It is resulting in Eq. (6).

$$rd = \frac{\left(\frac{(Ft_{bst}^{*}{}^{1.5})}{Ft_{wst}}\right)}{N_p} \tag{6}$$

Now, the population count is provided as N_p, the best and poor fitness functions (FF) are called Ft_{bst} and Ft_{wst} , the random function is described as rd and this randomly formed number when utilized in the Eq. (7).

$$A_b = a_{b,c} + rd.(UB_c - LB_c), b = 1,2,\cdots,B, c = 1,2,\cdots d \tag{7}$$

The random actual number resulting in Eq. (6) is named rd, the lower and upper limits on the c^{th} decision variables are represented as LB_c and UB_c, the coatis count is specified as B, the decision variables counts is characterized as d, the value of c^{th} decision variable is represented as $a_{b,c}$ and the position of b^{th} coati on the search area is provided as A_b. The pseudo-code for the recently designed MUCOA method.

Algorithm 1: Pseudocode of MUCOA
Information on optimizer problems is serves as input.
Parameters are initialized
First parameters are generated and the objective function is established.
The iguana position is upgraded.
if $b > \frac{B}{2}$ then
Calculate the random number utilizing Eq. (7)
Create the iguana location depending on the updated randomly generated number.
End if
Save the optimal candidate solution
End

The MUCOA initiates an FF to acquire better performance of classification. It establishes a progressive number to epitomize the superior performance of the candidate solutions. In this work, the reduction of the classifier error rate was measured as the FF, as provided in Eq. (8).

$$fitness(x_i) = ClassifierErrorRate(x_i) = \frac{no\ of\ misclassified\ samples}{Total\ no\ of\ samples} \times 100 \tag{8}$$

4. Experimental Validation

This article studies the performance of the COAPT-PWTLM technique on two datasets such as UCSDPed1 [22] and UCSDPed2 [23] datasets. Table 1 represents the detailed description on two datasets.

Table 1: Dataset description

Dataset	No. of Videos	Training Set	Testing Set	Average Frames	Dataset Length
"UCSDPed1 (Bikers, small carts, walking across walkways)"	70	34	36	201	5 min
"UCSDPed2 (Bikers, small carts, walking across walkways"	28	16	12	163	5 min

In Fig. 3, the TRA $accu_y$ (TRAAY) and validation $accu_y$ (VLAAY) performances of the COAPT-PWTLM technique based on UCSDPed1 dataset is illustrated. The figure highlighted that the TRAAY and VLAAY values expresses a cumulative propensity, illustrating the competency of the COAPT-PWTLM approach with improved performance through diverse iterations. Moreover, the TRAAY and VLAAY ruins nearer across the epochs, which notified diminish overfitting and presents superior outcome of the COAPT-PWTLM approach, assuring steady prediction on unnoticed samples.

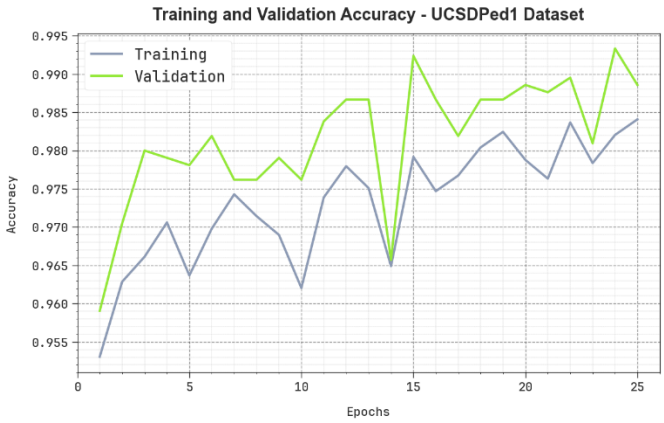

Figure 3. $Accu_y$ curve of COAPT-PWTLM approach at UCSDPed1 dataset

In Fig. 4, the TRA loss (TRALO) and VLA loss (VLALO) graph of the COAPT-PWTLM approach is illustrated. The decreasing TRALO and VLALO values indicate that the COAPT-PWTLM approach effectively balances generalization and data fitting. This reduction in loss reflects improved performance and progressively refined results.

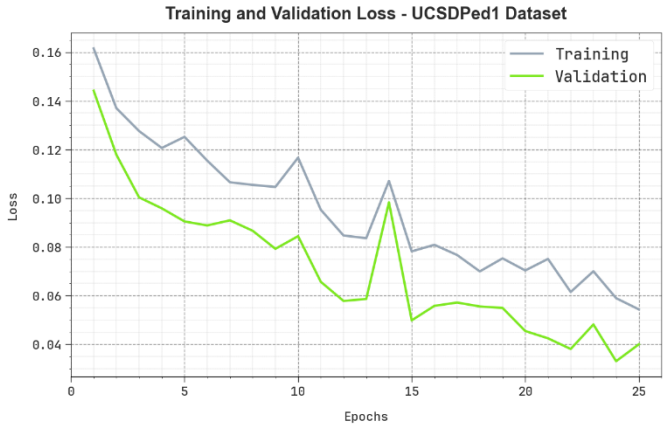

Figure 4. Loss curve of COAPT-PWTLM approach at UCSDPed1 dataset

In Table 2 and Fig. 5, brief comparative results of the COAPT-PWTLM method through existing techniques under UCSDPed1 dataset are portrayed [24]. The table values imply that COAPT-PWTLM method has outperformed that better performances compared to other models. On 5 false positive rate (FPR), the COAPT-PWTLM model obtained higher true positive rate (TPR) of 0.6570 while the MPPCA, SF, MDT, AMDN, EADN, and ADPW-FLHHO approaches achieved lesser TPR of 0.1034, 0.2420, 0.2327, 0.3404, 0.3567, and 0.6060. In addition, on 45 FPR, the COAPT-PWTLM technique gained higher TPR of 1.0000 whereas the MPPCA, SF, MDT, AMDN, EADN, and ADPW-FLHHO approaches accomplished minimal TPR of 0.7674, 0.8963, 0.8920, 0.9480, 0.9808, and 0.9994.

Table 2: Comparative outcome of COAPT-PWTLM approach with existing models under UCSDPed1 dataset

TPR							
FPR	MPPCA	Social Force	MDT	AMDN	EADN	ADPW-FLHHO	COAPT-PWTLM
0	0.0000	0.0000	0.0000	0.0000	0.0000	0.0000	0.0000
5	0.1034	0.2420	0.2327	0.3404	0.3567	0.6060	0.6570
10	0.2427	0.4160	0.4060	0.4560	0.5662	0.7585	0.8305
15	0.3570	0.5140	0.5113	0.5812	0.7688	0.8305	0.9015
20	0.4415	0.6010	0.5920	0.7042	0.7679	0.8876	0.9656
25	0.9474	0.7679	0.7647	0.6900	0.5456	0.5345	0.6105
30	0.5859	0.7741	0.7614	0.8569	0.9566	0.9689	0.9747
35	0.6398	0.8100	0.8013	0.9159	0.9728	0.9868	0.9948
40	0.6953	0.8600	0.8648	0.9426	0.9716	0.9930	0.9993
45	0.7674	0.8963	0.8920	0.9480	0.9808	0.9994	1.0000
50	0.8097	0.9406	0.9341	0.9764	0.9913	0.9896	0.9975
55	0.8390	0.9757	0.9696	0.9862	0.9819	0.9907	0.9978
60	0.8852	0.9790	0.9812	0.9853	0.9885	0.9999	1.0000
65	0.9191	0.9851	0.9822	0.9905	0.9946	0.9870	1.0000
70	0.9619	0.9876	0.9970	0.9956	0.9991	1.0000	1.0000
75	0.9692	0.9846	0.9844	0.9904	0.9991	1.0000	1.0000
80	0.9784	0.9870	0.9971	1.0000	1.0000	1.0000	1.0000
85	0.9836	0.9996	1.0000	1.0000	1.0000	1.0000	1.0000
90	0.9995	0.9982	1.0000	1.0000	1.0000	1.0000	1.0000
95	0.9940	1.0000	1.0000	1.0000	1.0000	1.0000	1.0000
100	1.0000	1.0000	1.0000	1.0000	1.0000	1.0000	1.0000

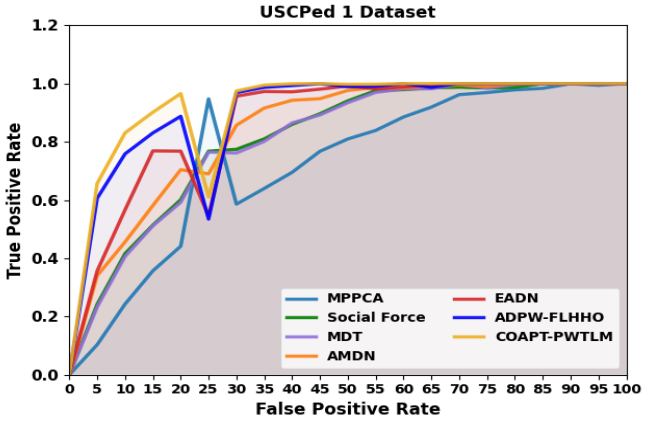

Figure 5. Comparative outcome of COAPT-PWTLM approach under UCSDPed1 dataset

In Table 3 and Fig. 6, the experimental AUC_{score} performances of the COAPT-PWTLM model with recent methodologies based on UCSDPed1 dataset are provided. The performances show that the TSN-RGB and Spatiotemporal techniques have revealed poorer performances with AUC_{score} of 90.55% and 91.63%, correspondingly. Simultaneously, the TSN-Optical Flow and MIL-C3D approaches have reached marginally enhanced solutions with AUC_{score} of 92.92% and 95.05%, correspondingly. Also, the Binary SVM and EADN approaches obtained discreetly nearer outcomes with AUC_{score} of 96.78% and 98.42%, correspondingly. At the same time, the ADPW-FLHHO method has proceeded in substantial solution with AUC_{score} of 99.42%. However the COAPT-PWTLM method outperforms the other approaches with higher AUC_{score} of 99.51%.

Table 3: AUC_{score} outcome of COAPT-PWTLM approach with other models under UCSDPed1 dataset

Models	AUC Score (%)
COAPT-PWTLM	99.51
ADPW-FLHHO	99.42
EADN	98.42
Binary SVM	96.78
MIL-C3D	95.05
TSN-Optical Flow	92.92
Spatiotemporal	91.63
TSN-RGB	90.55

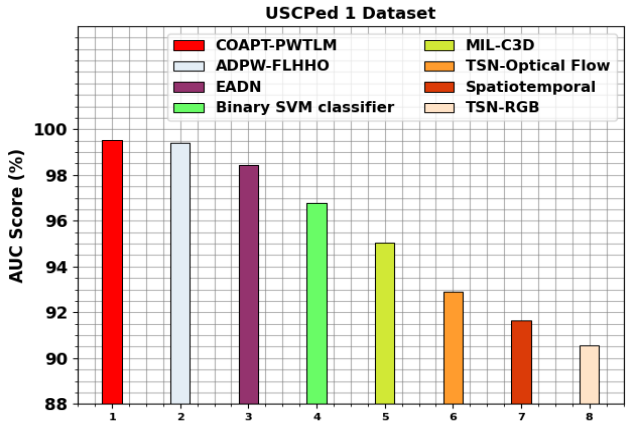

Figure 6. AUC_{score} outcome of COAPT-PWTLM technique under UCSDPed1 dataset

In Fig. 7, the TRAAY and VLAAY performances of the COAPT-PWTLM technique based on UCSDPed2 dataset are depicted. The figure highlights that TRAAY and VLAAY values exhibit an increasing trend, illustrating the capability of the COAPT-PWTLM model to achieve high performance over multiple iterations. Their convergence across epochs indicates reduced overfitting and stable prediction on unseen data.

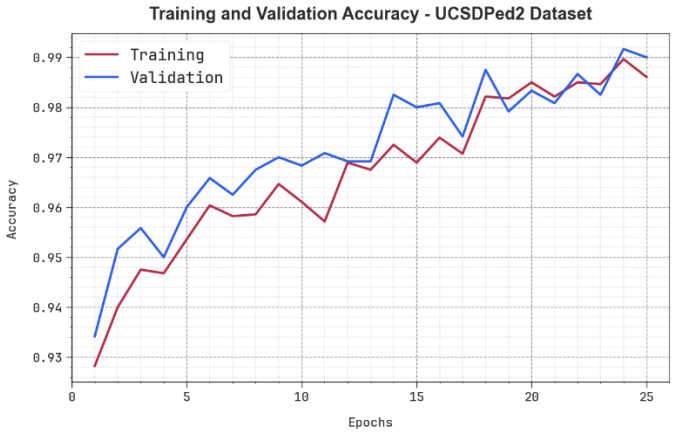

Figure 7. $Accu_y$ Curve of COAPT-PWTLM approach at UCSDPed2 dataset

In Fig. 8, the TRALO and VLALO graph of the COAPT-PWTLM method is depicted. The diminishing TRALO and VLALO values illustrate the efficiency of the COAPT-PWTLM technique in balancing generalization and data fitting. The steady decline in loss confirms improved performance and gradually refines the prediction accuracy of the model.

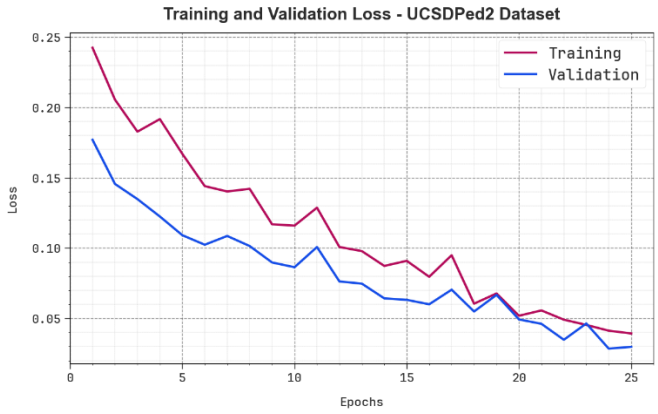

Figure 8. Loss curve of COAPT-PWTLM approach at UCSDPed2 dataset

In Table 4 and Fig. 9, a brief comparison analysis of the COAPT-PWTLM method through existing models based on UCSDPed2 dataset is exposed. The values of table indicate that COAPT-PWTLM method has outperformed that greater performances related to other techniques. With 5 FPR, the COAPT-PWTLM methodology attained maximum TPR of 0.4463 whereas the MPPCA, SF, MDT, AMDN, EADN, and ADPW-FLHHO models obtained diminish TPR of 0.0820, 0.1391, 0.2701, 0.3898, 0.3603, and 0.3723. Furthermore, on 45 FPR, the COAPT-PWTLM method attained maximum TPR of 0.9937 whereas the MPPCA, SF, MDT, AMDN, EADN, and ADPW-FLHHO models reached minimum TPR of 0.8097, 0.9363, 0.8863, 0.9482, 0.9611, and 0.9770.

Table 4: Comparative outcome of COAPT-PWTLM methodology with existing models under UCSDPed2 dataset

TPR							
FPR	MPPCA	Social Force	MDT	AMDN	EADN	ADPW-FLHHO	COAPT-PWTLM
0	0.0000	0.0000	0.0000	0.0000	0.0000	0.0000	0.0000
5	0.0820	0.1391	0.2701	0.3898	0.3603	0.3723	0.4463
10	0.2514	0.2808	0.4371	0.4815	0.5467	0.5638	0.6428
15	0.3675	0.4294	0.5606	0.5466	0.6140	0.6250	0.6770
20	0.4964	0.5056	0.6487	0.6896	0.7494	0.7614	0.8134
25	0.5691	0.6653	0.7714	0.6976	0.7883	0.7969	0.8469
30	0.6928	0.7549	0.8022	0.8745	0.9286	0.9343	0.9913
35	0.7252	0.8483	0.8104	0.9248	0.9509	0.9668	0.9836
40	0.7776	0.8974	0.8367	0.9373	0.9576	0.9647	0.9797
45	0.8097	0.9363	0.8863	0.9482	0.9611	0.9770	0.9937
50	0.8380	0.9604	0.9411	0.9665	0.9771	0.9849	1.0000
55	0.9370	0.9667	0.9733	0.9797	0.9862	0.9981	1.0000
60	0.9495	0.9803	0.9806	0.9912	0.9849	1.0000	1.0000
65	0.9557	0.9952	0.9998	0.9980	0.9953	1.0000	1.0000
70	0.9709	1.0035	1.0000	0.9967	0.9961	1.0000	1.0000
75	0.9914	0.9904	1.0000	0.9978	0.9991	1.0000	1.0000
80	0.9908	0.9985	1.0000	0.9984	1.0000	1.0000	1.0000
85	0.9884	0.9978	1.0000	1.0000	1.0000	1.0000	1.0000
90	1.0000	1.0000	1.0000	1.0000	1.0000	1.0000	1.0000
95	1.0000	1.0000	1.0000	1.0000	1.0000	1.0000	1.0000
100	1.0000	1.0000	1.0000	1.0000	1.0000	1.0000	1.0000

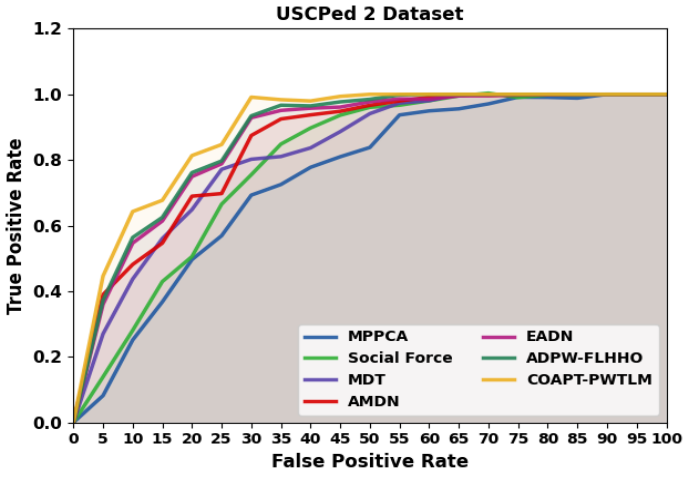

Figure 9. Comparative outcome of COAPT-PWTLM methodology under UCSDPed2 dataset

In Table 5 and Fig. 10, the AUC_{score} performances of the COAPT-PWTLM model with recent methodologies based on UCSDPed2 dataset are specified. The performances show that the TSN-RGB and Spatiotemporal methods have displayed poorer performances with AUC_{score} of 90.51% and 92.53%, correspondingly. Simultaneously, the TSN-Optical Flow and MIL-C3D techniques have gained marginally improved solutions with AUC_{score} of 94.4% and 95.57%, subsequently. Moreover, the Binary SVM and EADN methods have reached judiciously nearer performances with AUC_{score} of 97.21% and 98.36%, correspondingly. Likewise, the ADPW-FLHHO model has resulted in significant results with AUC_{score} of 99.26%. Nevertheless, the COAPT-PWTLM model outperforms the other techniques with improved AUC_{score} of 99.31%.

Table 5: AUC_{score} outcome of COAPT-PWTLM technique with other models under UCSDPed2 dataset

Technique	AUC Score (%)
COAPT-PWTLM	99.31
ADPW-FLHHO	99.26
EADN	98.36
Binary SVM	97.21
MIL-C3D	95.57
TSN-Optical Flow	94.41
Spatiotemporal	92.53
TSN-RGB	90.51

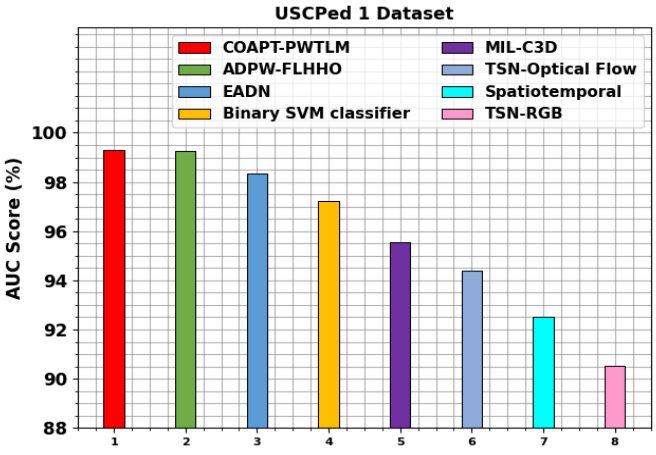

Figure 10. AUC_{score} Outcome of COAPT-PWTLM approach under UCSDPed2 dataset

5. Conclusion

In this paper, the COAPT-PWTLM technique is proposed. The main goal of COAPT-PWTLM technique is to provide automatic detection of pedestrian walkways for disability using advanced models. Initially, the MF is utilized in the image pre-processing stage for eliminating the noise from an input image data. Furthermore, the SquezeNet1.1 model is employed for feature extraction. For the classification process, the COAPT-PWTLM technique utilizes the MLAE model. Finally, the MUCOA adjusts the hyperparameter range of MLAE model optimally and results in improved classification performance. The experimental validation of the COAPT-PWTLM approach is verified on benchmark image dataset and the outcome are evaluated under dissimilar measures. The experimental outcome underlined the progress of the COAPT-PWTLM approach over the existing models.

Data Availability Statement: The data that support the findings of this study are openly available in Kaggle repository at http://www.svcl.ucsd.edu/projects/anomaly/dataset.htm, and http://www.cse.cuhk. edu.hk/ leojia/ projects/detectabnormal/dataset.html references number [22, 23].

Funding: “This research received no external funding”

Conflicts of Interest: “The authors declare no conflict of interest.”

References

[1] S. Gamache, F. Routhier, E. Morales, M. H. Vandersmissen, and N. Boucher, "Mapping review of accessible pedestrian infrastructures for individuals with physical disabilities," *Disability and Rehabilitation: Assistive Technology*, vol. 14, no. 4, pp. 410–422, 2019.

[2] R. Machingaidze, "Road Safety and Accessibility: Facilitating the autonomous movement of people with physical disabilities in pedestrian environments," 2021.

[3] P. K. Odame and R. O. Amoako-Sakyi, "Sidewalk accessibility and pedestrian safety among students with physical disability in the University of Cape Coast," *Current Res. J. Soc. Sci. & Human.*, vol. 2, p. 109, 2019.

[4] X. Zheng, "Accessibility and Usability in the City of Malmö: Assessing the Implementation of Universal Design on Pedestrian Walkways for the Blind and Visually Impaired," 2023.

[5] M. Wojnowska-Heciak, J. Heciak, and A. Kłak, "Perceptions of street trees among Polish residents with motor disabilities," *Journal of Transport & Health*, vol. 27, p. 101490, 2022.

[6] U. I. Badawy, M. Q. Jawabrah, and A. Jarada, "Adaptation of accessibility for people with disabilities in private and public buildings using appropriate design checklist," *International journal for modern trends in science and technology*, 2020.

[7] B. A. Piskin and N. S. Akdeniz, "How Can People with Disabilities Use the Outdoors? An Assessment Within the Framework of Disability Standards," *Social Indicators Research*, vol. 167, no. 1, pp. 153–174, 2023.

[8] P. N. Hashim *et al.*, "A Study on the Disabled Facilities and Persons with Disabilities (PWDs) Customers' Satisfaction in Sunway Pyramid," *Journal of Built Environment, Technology and Engineering*, vol. 8, pp. 84–100, 2020.

[9] Weaver III *et al.*, "Pedestrian Walkways: Hidden Hazards Related to Common Landscaping Practices," *Professional Safety*, vol. 67, no. 07, pp. 14–22, 2022.

[10] K. A. Alhassan, M. F. A. Rahman, and S. K. A. Kadir, "A comprehensive review of smart mobility solutions for individuals with disabilities," *Journal of Traffic and Transportation Engineering*, vol. 12, no. 4, pp. 225–240, 2023.

[11] M. Talaat *et al.*, "Intelligent wearable vision systems for the visually impaired in Saudi Arabia," *Neural Computing and Applications*, pp. 1–21, 2025.

[12] S. S. Nasabeh, S. Meliá, B. Leporini, and D. Gadzhimusieva, "Empowering Visual Navigation: A Deep-Learning Solution for Enhanced Accessibility and Safety Among the Visually Impaired," in *International Conference on Web Information Systems Engineering*, Singapore: Springer Nature Singapore, Nov. 2024, pp. 338–348.

[13] Jeong, K. Kim, J. Jung, and J. Cho, "YOLOv8-Based XR Smart Glasses Mobility Assistive System for Aiding Outdoor Walking of Visually Impaired Individuals in South Korea," *Electronics*, vol. 14, no. 3, p. 425, 2025.

[14] R. I. Chowdhury, J. Anjom, and M. I. A. Hossain, "A novel edge intelligence-based solution for safer footpath navigation of visually impaired using computer vision," *Journal of King Saud University-Computer and Information Sciences*, vol. 36, no. 8, p. 102191, 2024.

[15] Choi, T. A. Dinh, and M. Choi, "Enhancing Driving Safety of Personal Mobility Vehicles Using On-Board Technologies," *Applied Sciences*, vol. 15, no. 3, 2025.

[16] J. Lee, K. A. Cha, and M. Lee, "Multi-Modal System for Walking Safety for the Visually Impaired: Multi-Object Detection and Natural Language Generation," *Applied Sciences*, vol. 14, no. 17, p. 7643, 2024.

[17] S. Ikram, I. Sarwar, A. Ikram, and M. Abdullah-AI-Wahud, "A Transformer-Based Multimodal Object Detection System for Real-World Applications," *IEEE Access*, 2025.

[18] V. Rathi, A. Sharma, and A. K. Singh, "Multispectral images reconstruction using median filtering based spectral correlation," *Image and Vision Computing*, p. 105462, 2025.

[19] S. B. Nettur *et al.*, "UltraLightSqueezeNet: A Deep Learning Architecture for Malaria Classification with up to 54x fewer trainable parameters for resource constrained devices," *arXiv preprint arXiv: 2501.14172*, 2025.

[20] N. Al-Kahtani *et al.*, "Discrete Migratory Bird Optimizer with Deep Transfer Learning Aided Multi-Retinal Disease Detection on Fundus Imaging," *Results in Engineering*, p. 104574, 2025.

[21] K. Thiraviam and R. Karthiyayini, "An Efficient Early-Onset Plant Disease Prediction using Improved Heuristic-aided Adaptive Ensemble Network with Leaf Image-based Phenotype Data: HEURISTIC ADAPTIVE ENSEMBLE IN PLANT DISEASE PREDICTION," *Journal of Scientific & Industrial Research (JSIR)*, vol. 84, no. 03, pp. 287–300, 2025.

[22] "Anomaly Dataset". [Online]. Available: http://www.svcl.ucsd.edu/projects/anomaly/dataset.htm. [Accessed: 17 Mar. 2025].

[23] "Abnormal Detection Dataset". [Online]. Available: http://www.cse.cuhk.edu.hk/leojia/projects/detectabnormal/dataset.html. [Accessed: 17 Mar. 2025].

[24] M. A. Alohali *et al.*, "Anomaly detection in pedestrian walkways for intelligent transportation system using federated learning and harris hawks optimizer on remote sensing images," *Remote Sensing*, vol. 15, no. 12, p. 3092, 2023.